

SOLUTION BEHAVIORS AND ADSORPTION CHARACTERISTICS OF SODIUM LIGNOSULFONATE UNDER DIFFERENT PH CONDITIONS

Yong Qian,^a Yonghong Deng,^a Conghua Yi,^a Haifeng Yu,^b and Xueqing Qiu^{a,*}

Solution behaviors and adsorption characteristics of sodium lignosulfonate (NaLS) were studied under different pH conditions. The changes of M_w and particle size of NaSL with solution pH were detected by laser light scattering (LLS). Film thickness was determined with a spectroscopic ellipsometer, and surface roughness was measured by atomic force microscopy (AFM). The results showed that NaSL aggregated in acidic water, and the degree of aggregation decreased with increasing pH. When solution pH increased, the M_w of NaLS decreased, indicating that the intermolecular aggregates of NaLS were disaggregated at high pH. In the meantime, the ratio of R_g/R_h decreased, suggesting that the intrastucture of NaSL was changed from compact to loose. When the NaSL with loose structure and low degree of aggregation was adsorbed on a solid substrate, the adsorption thickness and the surface roughness decreased correspondingly.

Keywords: Lignosulfonate; Aggregation; Conformation; Adsorption; pH

Contact information: a: State Key Lab of Pulp and Paper Engineering, School of Chemistry and Chemical Engineering, South China University of Technology, 381 Wushan Road, Guangzhou, 510640, China;

b: Top Runner Incubation Center for Academia-Industry Fusion, and Department of Materials Science and Technology, Nagaoka University of Technology, 1603-1 Kamitomioka, Nagaoka 940-2188, Japan.

* Corresponding author: cexqqiu@scut.edu.cn

INTRODUCTION

Lignosulfonate is a byproduct in the waste liquor from sulfite pulp mills. During the sulfite pulping process, the hydrophobic lignin is sulfonated and fragmented, becoming water soluble (Fredheim et al. 2003). Besides sulfonic groups, lignosulfonate contains carboxyl and phenolic hydroxyl groups too. Lignosulfonate is made up of different phenylpropanoid monomers, together with some functional groups. Lignosulfonate products have been used as anionic surfactants in various application areas, such as concrete water reducers, dispersants for water-coal-slurry, corrosion and scale inhibitors, and pesticide dispersants. Such uses have benefited from its favorable wettability, adsorptivity, and dispersive ability (Ouyang et al. 2009; Zhou et al. 2007; Ouyang et al. 2006; Li et al. 2009). The applied performance of lignosulfonate depends on the adsorption characteristics of lignosulfonate at solid-liquid interfaces.

The adsorption behaviors of lignosulfonate have been widely applied in systems involving coal/water, air/liquid interfaces, and metallic oxides (Zhang et al. 2005; Gundersen et al. 2001; Ratinac et al. 2004; Fagerholm et al. 1996). It is well known that NaLS becomes aggregated in acidic water, and the degree of aggregation decreases with increasing pH, which affects the adsorption behaviors of NaLS. However, the

aggregation state and the molecular conformation of NaLS in solutions of different pH and in solid films has not been fully understood up to this point.

In our previous paper we have studied the adsorption and desorption behaviors of sodium lignosulfonate (NaLS) on quartz slides at different pH using a layer-by-layer self-assembly method (Deng et al. 2010). In this paper, we investigated the relationship between the solution behaviors and the adsorption characteristics of NaLS by laser light scattering (LLS), ellipsometer, and AFM. The related work will be helpful to understand the aggregation state and molecular conformation of NaLS with different pH in solutions and in solid films.

EXPERIMENTAL

Materials

Sodium lignosulfonate, obtained from Shixian Papermaking Co. Ltd (China), was purified and fractionated through filtration, ultrafiltration, and gel column chromatography. NaLS was eluted from Sephacryl S-100 with water and 0.2 M sodium chloride solution. The rate of elution in the column was 5 mL/min. The fractions were eluted from Sephadex LH-20 with water as the mobile phase to remove sodium chloride according to the theories of size exclusion, ionic repulsion, and physical adsorption. A NaLS fraction with low polydispersity index was then obtained as described by Ouyang et al. (2010). The contents of the sulfonic, carboxyl, and phenolic groups were measured to be 9.28 wt%, 3.87 wt%, and 1.59 wt%, respectively (Deng et al. 2010). Milli-Q water (resistivity $> 18 \text{ M}\cdot\text{cm}^{-1}$) used in the experiment was obtained from a Millipore water purification system. Poly-(diallyldimethylammonium chloride) (PDAC) with molecular weight (M_w) ranges from 200,000 to 350,000 was purchased from Aldrich. NaCl and other reagents were purchased commercially as analytical grade products from Sinopharm Chemical Reagent Co. Ltd. (China). The NaLS was clarified with a 0.45 μm Millipore Millex-LRC filter to remove dust before the LLS measurement.

Characterization

A commercial light scattering spectrometer (ALV/CGS-3, ALV, Germany) equipped with a multi- τ digital time correlation (LSE-5004, ALV, Germany) and a cylindrical 22 mW Uniphase He-Ne laser ($\lambda_0=632 \text{ nm}$) as the light source was used. The dn/dc value of NASL was determined by BI-DNDC (DNDC-2010, WEG, Germany). A 632.8 nm interference filter and a Glan-Thompson interferometer were used to avoid overestimation of the molecular weight of NASL due to fluorescence and polarization. The NASL solution is so dilute that the adsorption effect could be neglected.

In classic (static) LLS, we can obtain the weight-average molecular weight (M_w), the root-mean square radius of gyration (R_g), and the second virial coefficient (A_2) of sodium lignosulfonate in aqueous solution from the angular and concentration dependence of the excess absolute scattering intensity, known as Zimm plot, on the basis of,

$$\frac{Kc}{R(\theta)} = \frac{1}{M_w} \left(1 + \frac{16\pi^2}{3\lambda^2} R_g^2 \sin^2 \frac{\theta}{2} + \dots \right) + 2A_2c \quad (1)$$

where $K=4\pi^2n^2(dn/dc)^2/(N_A\lambda_0^4)$ with N_A , dn/dc , n , and λ_0 being the Avogadro number, the specific refractive index increment, the solvent refractive index, and the wavelength of the light in vacuum, respectively.

In dynamic LLS, the measured intensity-intensity-time correlation function $G^{(2)}(q, t)$ and electric field-field-time correlation function $g^{(1)}(q, t)$ has a relationship as follows,

$$G^{(2)}(q, t) = A[1 + \beta |g^{(1)}(q, t)|^2] \quad (2)$$

where A , β , and τ are the test baseline, instrument correlation factor, and delay time, respectively. In a polydisperse system, the relationship between $G^{(1)}(\tau)$ and line-width distribution $G(\Gamma)$ is:

$$g^{(1)}(q, t) = \int_0^\infty G(\Gamma)e^{-\Gamma t} d\Gamma \quad (3)$$

By Laplace inversion, we can get $G(\Gamma)$. For a diffusive relaxation, Γ is related to the translational diffusion coefficient D by $(\Gamma/q^2)_{q \rightarrow 0} = D$; therefore $G(\Gamma)$ can be converted into a hydrodynamic radius distribution $f(R_h)$ via the Stokes-Einstein equation, $R_h = k_B T / 6\pi\eta D^{-1}$, where k_B , T , and η are the Boltzmann constant, the absolute temperature, and the solvent viscosity, respectively.

An alternative method of analyzing the more complicated data obtained from a polydisperse sample in a quantitative way is the so-called ‘‘cumulant analysis’’, which is based on a series expansion of $g^{(1)}(q, t)$. The details of the analysis can be seen in the book by Schartl (2007). In this work, we fit the decay line of five angles (30° , 60° , 90° , 120° , 150°) by the ‘‘cumulant analysis’’ method, and extrapolate to angle 0 to obtain the R_h of a certain concentration.

The molecular weight distribution of the NaLS sample was determined by using aqueous gel permeation chromatography (GPC) with Ultrahydrogel 120 and Ultrahydrogel 250 columns. The mobile phase was 0.1 M NaNO_3 and the pH was adjusted to the range 8.0 to 8.5 by adding NaOH. The effluent was monitored at 280 nm with a Waters 2487 UV Absorbance Detector (Waters Corp., USA).

Film thickness was determined with a spectroscopic ellipsometer (UVISEL-NIR-FGMS, Horiba).

The morphological images were observed using an AFM (Nanoscope IIIa multimode, Veeco Co., USA) by the tapping mode.

Fabrication of Self-Assembled Film

The NaLS/PDAC layer-by-layer (LBL) self-assembled films of desired bilayers were deposited on quartz slide substrates ($50 \times 14 \times 8$ mm). Prior to deposition, the quartz slide was sonicated in a 98% $\text{H}_2\text{SO}_4/30\%\text{H}_2\text{O}_2$ solution (piranha solution) for 1 h and in a $\text{H}_2\text{O}/\text{H}_2\text{O}_2/\text{NH}_4\text{OH}$ (5:1:1) solution for 1 h, followed with a thorough rinsing, and then dried with an air stream. The film deposition process involved the repeated sequential dipping of the substrate into the polycation (PDAC) and polyanion (NaLS) solutions for

10 minutes. The slide was thoroughly rinsed with Milli-Q water and blown dry with air between each of the deposition steps.

RESULTS AND DISCUSSION

Solution Behaviors of NaLS

NaLS used here was carefully purified through filtration, ultrafiltration, and gel column chromatography. A NaLS fraction with narrow M_w distribution was obtained through the method of gel column chromatographic separation as described by Ouyang et al. (2010). The polydispersity index of M_w of NaLS fraction was measured to be 1.2 by GPC. The molecular weight, particle size, and the effect of pH on the solution behaviors of NaLS were investigated by LLS, as described in the following sections.

Light scattering measurement

Figure 1 is the Zimm plot of NaLS solutions. The following static parameters were obtained: $M_w = 4.858 \times 10^5$ g/mol, $R_g = 67.21$ nm, and $A_2 = 1.557 \times 10^{-6}$ mol·dm³/g². The “overlap” concentration c^* is estimated to be 0.846 g/L, calculated from $\langle R_g \rangle$, M_w , and Avogadro’s number N_A based on the “dilute-semi-dilute” critical changing concentration formula: $c^* = 3M_w / (4\pi R_g^3 N_A)$. Figure 2 shows the normalized intensity correlation function $g^{(2)}(t)$ of NaLS versus delay time t , measured at different angles. The hydrodynamic radius $\langle R_h \rangle$ was determined to be 66.49 nm by extrapolation of the effective R_h obtained from “cumulant analysis” towards zero scattering angle (Fig. 2b).

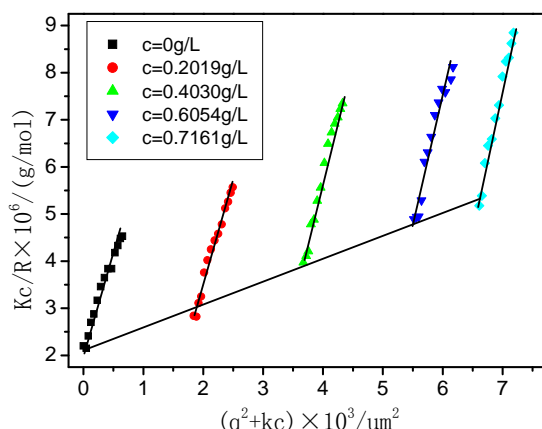


Fig. 1. Zimm plot for NaLS in water (pH=7). The concentrations of four NaLS solutions were 0.2019 g/L, 0.4030 g/L, 0.6054 g/L, and 0.7161g/L. The black square symbols correspond to the values of Kc/R of concentration zero.

It is well known that the ratio of radius of gyration to hydrodynamic radius (R_g/R_h) is related to the spatial density distribution and the degree of draining of a scattering object in solution or dispersion (Nie et al. 2003; Schärfl 2007). In Fig. 3, the R_g/R_h values of NaLS with different concentration lie in the range of 1.0 to 1.1, indicating that NaLS has a loose spherical structure in water, which is in accordance with the conformation model presented by Qiu et al. (2010).

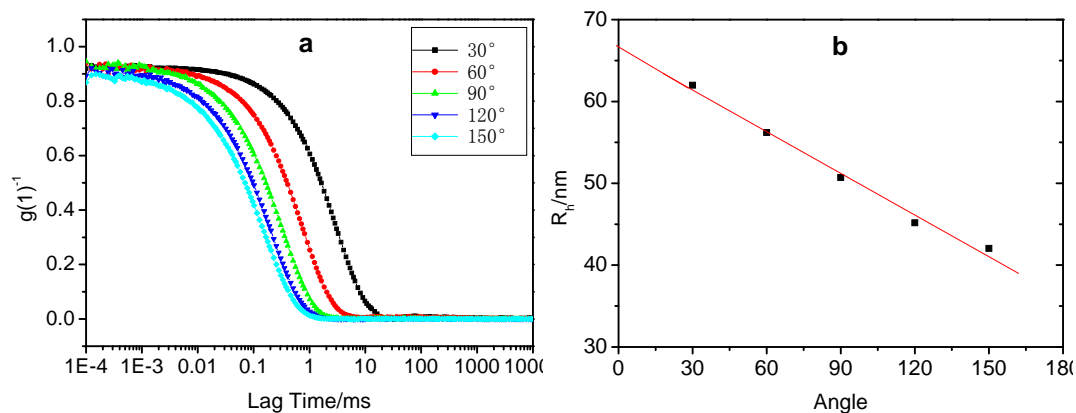


Fig. 2. (a) Normalized intensity correlation function $g^{(2)}(t)$ of NaLS versus lag time, measured at different angles; (b) The hydrodynamic radius $\langle R_h \rangle$, determined by extrapolation of the effective R_h towards zero scattering angle

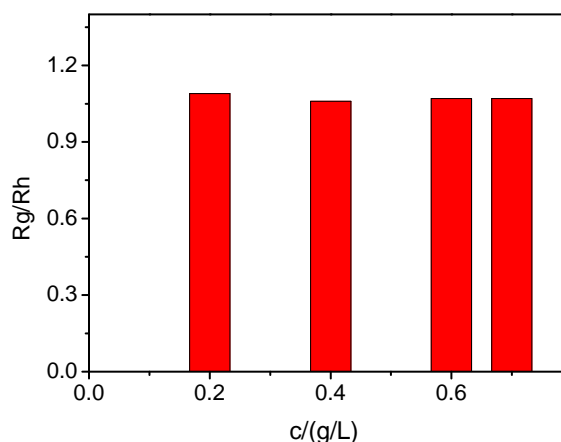


Fig. 3. R_g/R_h columns of NaLS with different concentration in water solution (pH=7). The experimental points are those included in Fig. 1.

Effect of pH on the solution behaviors

The dn/dc values of NaLS at pH 6.88, 10.01, and 13.26 were measured to be 0.202, 0.212, and 0.242, respectively. As BI-DNDC couldn't evaluate the dn/dc values at low pH, the dn/dc values at acidic condition were regarded as 0.202. Figure 4 shows the M_w of NaLS as a function of the solution pH values. The M_w of NaLS decreases with increasing solution pH, and exhibits two inflections. The first inflection of M_w is near pH 3.98. When pH is changed from 3.01 to 3.98, the M_w of NaLS is changed from 4.779×10^5 to 3.322×10^5 g/mol. The second inflection is near pH 9.42. When pH is changed from 9.42 to 12.26, the M_w is changed from 2.958×10^5 to 1.384×10^5 g/mol. This phenomenon is caused by the specific molecular structure and the configuration characteristics. The larger M_w of NaLS under the lower pH conditions may be attributed to molecular aggregation due to lower ionization degree. The first inflection point of M_w near pH 3.98 is related to the ionization of carboxylic groups, while the second inflection near pH 9.42 is related to the ionization of phenolic groups. The two ionized points are in agreement with the potentiometric titration results (Deng et al. 2010). Woerner et al. (1988) have investigated the association of the kraft lignin, and concluded that protona-

tion of phenolic hydroxyl groups was the controlling step of association. In our case, the protonation of carboxylic groups and phenolic hydroxyl groups are the controlling steps of association, resulting in two inflection points of M_w .

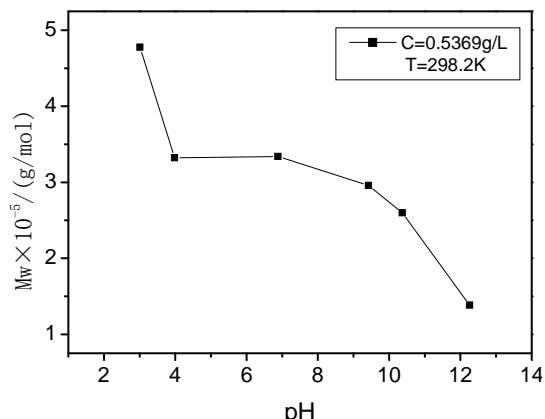


Fig. 4. Apparent molecular weight (M_w) of NaLS as a function of the solution pH values at 298K. The concentration of NaLS is 0.5369g/L.

In Fig. 5, the R_g/R_h plot, which is related to the conformation, also has two inflections. From pH 2.42 to pH 3.98, R_g/R_h is changed from 0.84 to 1.12, which indicates that the conformation of NaLS aggregations swelled from a comparatively compact to loose structure. It can be explained that the electrostatic repulsion gets stronger when carboxylic groups inside the particle are ionized. At the second inflection, the phenolic groups are ionized at pH 9.38. The loose structure becomes more stretched, and the distance between hydrophobic bonds of NaLS monomers is even larger. The loose swelling conformation is easy to collapse when the NaLS is dried on a substrate such as quartz slide.

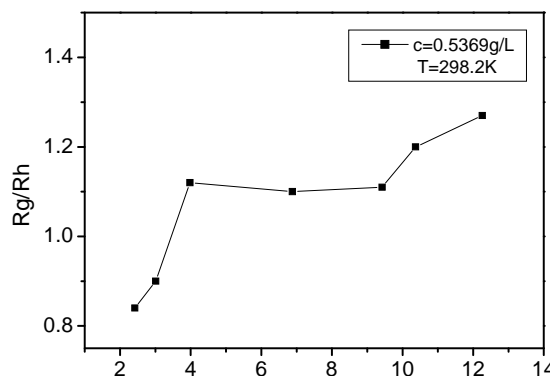


Fig. 5. R_g/R_h values of NaLS as a function of the solution pH values at 298K. The concentration of NaSL is 0.5369 g/L.

Adsorption Behaviors of NaLS with Different pH

To explore the effect of pH on the adsorption characteristic of NaLS, NaLS/PDAC layer-by-layer self-assembled multilayer films were prepared from NaLS solutions with five pH values. Table 1 shows the film thickness of the 10-bilayer

NaLS/PDAC multilayers obtained from NaLS solutions with different pH. When pH is changed from 2.12 to 5.10, the thickness decreases sharply from 75.6 nm to 14.4 nm. As pH further increases, the thickness decreases gradually. This phenomenon is in accordance with the previous study on the adsorption behaviors characterized by UV-vis spectroscopy (Deng et al. 2010). Since the M_w of NaLS decreases with increasing pH, it is reasonable that the adsorption amount of NaLS decreases with increasing pH (Zhang et al. 2005; Qiu et al. 2003).

Table 1. Film Thickness and Surface Roughness of 10-bilayer NaLS/PDAC Multilayers Obtained from NaLS Solution with Different pH

Solution pH	Film thickness (nm)	Surface roughness (nm)
2.12	75.6	2.2
3.01	41.3	2.0
5.10	14.4	0.9
9.97	5.6	0.6
12.04	5.0	0.4

Atomic force microscopy (AFM) is a powerful tool to probe surface morphology and microstructure characteristics. Figure 6 shows AFM images of 10-bilayer NaLS/PDAC self-assembly film with NaLS as the outmost layer. At pH 3.01, sphere-like particles were observed on the film surface, and the film roughness was calculated to be 2.0 nm. At pH 12.04, a very smooth surface was obtained because NaLS had a loose swollen structure. The dried film had an averaged roughness of 0.4 nm. The surface roughness of NaLS film prepared at pH 5.10 was 0.9 nm, which is in between 2.0 and 0.4 nm. Obviously, the surface roughness decreases with increasing pH (Table 1).

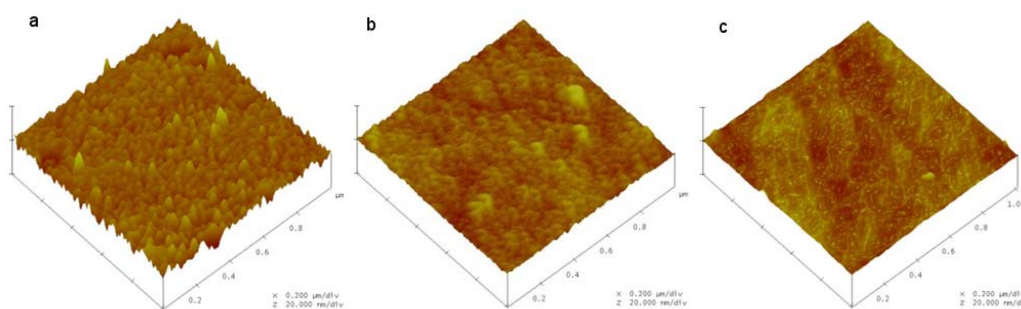


Fig. 6. AFM images of 10-bilayer NaLS/PDAC self-assembly film with NaLS as the outmost layer. (a) pH = 3.01; (b) pH = 5.10; (c) pH = 12.04.

Aggregation State and Molecular Conformation of NaLS

According to the solution behaviors and the adsorption characteristics of NaLS, we propose an aggregation state and molecular conformation of NaLS in water and at solid-liquid interface (Fig. 7). NaLS consists of hydrophobic phenyl-propanoid groups (e.g. guaiacyl, syringyl, and p-hydrophenyl) and hydrophilic functional groups (e.g.

sulfonic, carboxyl, and phenolic hydroxyl groups). In acidic solutions, NaLS exists as compact aggregates with the hydrophobic phenyl-propanoid groups as the cores and the hydrophilic functional groups as the shells. At a lower pH, when these compact NaLS aggregates are adsorbed on PDAC and then dried, a thicker self-assembled film with higher surface roughness is obtained (Fig. 6a, Table 1).

By contrast, in basic solutions, both the carboxyl and the phenolic hydroxyl groups are ionized, and then the M_w of NaLS decreases significantly, demonstrating that the NaLS aggregates are disaggregated. The corresponding R_g/R_h also increases, indicating that the conformation of NaLS macromolecules is changed from a comparatively compact to loose structure. When such NaLS macromolecules with a well-swollen structure are adsorbed on PDAC, a thinner self-assembled film with lower surface roughness is obtained (Fig. 6c, Table 1).

In neutral solutions, the carboxyl groups are ionized, but the phenolic hydroxyl groups are not ionized. The degree of aggregation for the intramolecular and intermolecular NaLS aggregates in neutral solutions is in between that in acidic and basic solutions. When the NaLS macromolecules are adsorbed on PDAC, the thickness and roughness of the NaLS/PDAC self-assembled film in neutral solutions are in between that in acidic and basic solutions.

The proposed model reflects the fact that the aggregation and conformation of NaLS changes with pH and the relationship between the solution behaviors and the adsorption characteristics of NaLS. The adsorption thickness and surface morphology depend on the aggregation state and molecular conformation of NaLS.

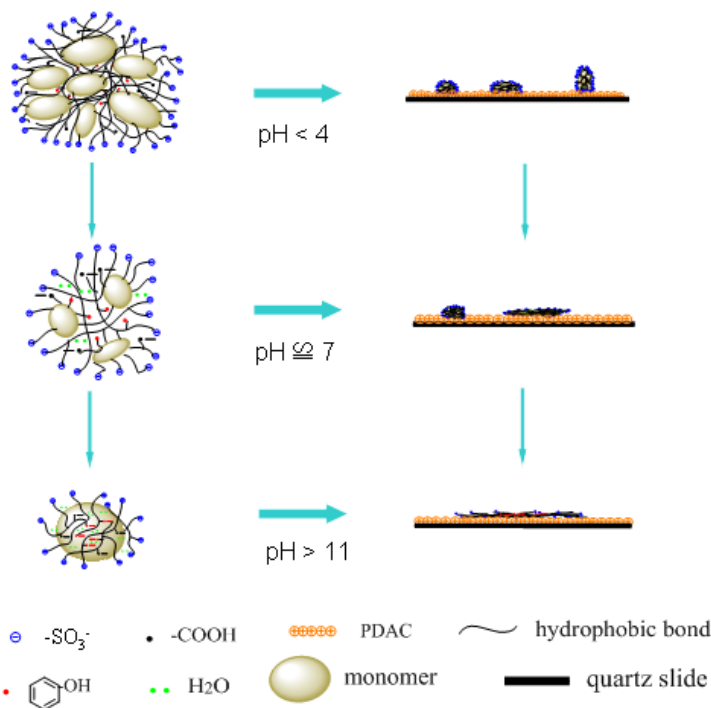


Fig. 7. The aggregation model of NaLS with different pH in water and at solid-liquid interface

The performance of lignosulfonates in various applications depends on their adsorption characteristics at solid-liquid interface, and the adsorption characteristics have a close relationship with the solution behaviors of lignosulfonates. Therefore, this study on the solution and adsorption behavior of lignosulfonate at different pH has both theoretical significance and application value. It not only gives a significant insight in understanding the conformation and aggregation of lignosulfonates, but also provides academic instruction that may be useful in the recovery of lignin from spent liquor for value-added applications.

CONCLUSIONS

1. In acidic solutions, NaLS existed as compact aggregates. When solution pH increased, the M_w of NaLS decreased, indicating that the intermolecular aggregates of NaLS were disaggregated at high pH. The corresponding R_g/R_h also increased, indicating that the conformation of NaLS macromolecules is changed from a comparatively compact to a loose structure.
2. When these NaLS aggregates were adsorbed on PDAC and then dried, the thickness and roughness of the NaLS/PDAC self-assembled film decreased with increasing pH because the intramolecular and intermolecular aggregates decreased.
3. The M_w and the R_g/R_h ratio of NaLS changed with increasing pH, and all exhibited two inflections. The first inflection was related to ionization of the carboxyl groups, and the second one was related to ionization of the phenolic hydroxyl groups.

ACKNOWLEDGMENTS

The authors thank the financial support of the China Excellent Young Scientist Fund (20925622), the National Natural Science Foundation of China (20976064, 21006036), and Science and Technology Projects of Guangdong Province of China (2009B050600004).

REFERENCES CITED

- Deng Y. H., Wu, Y., Qian, Y., Ouyang, X. P., Yang, D. J., and Qiu, X. Q. (2010). "Adsorption and desorption behaviors of lignosulfonate during the self-assembly of multilayers," *BioResources* 5(2), 1178-1196.
- Fagerholm, H., Johansson, L.-S., and Graeffe, M. (1996). "Surface charge and viscosity of mixed $\text{Si}_3\text{N}_4\text{-Y}_2\text{O}_3$ suspensions containing lignosulphonate," *J. Eur. Ceram. Soc.* 16, 671-678.
- Fredheim, G. E. (2003). "Polyelectrolyte complexes: Interactions between lignosulfonate and chitosan," *Biomacromolecules* 4(2), 232-239.
- Gundersen, S. A., Ese, M.-H., and Sjöblom, J. (2001). "Langmuir surface and interface films of lignosulfonates and kraft lignins in the presence of electrolyte and

- asphaltenes: Correlation to emulsion stability,” *Colloids Surf. A: Physicochemical and Engineering Aspects* 182, 199-218.
- Li, Z. L., Pang, Y. X., Lou, H. M., and Qiu, X. Q. (2009). “Influence of lignosulfonates on the properties of dimeethomorph water-disperse granules,” *BioResources* 4(2), 586-601.
- Nie, T., Zhao, Y., Xie, Z. W., Wu, Q. (2003). “Micellar formation of poly(caprolactone-block-ethylene oxide-block-caprolactone) and its enzymatic biodegradation in aqueous dispersion,” *Macromolecules* 36(23), 8825-8829.
- Ouyang, X. P., Ke, L. X., Qiu, X. Q., Guo, Y. X., and Pang, Y. X. (2009). “Sulfonation of alkli lignin and its potential use in dispersant for cement,” *J. Dispersion Sci. Technol.* 30(1), 1-6.
- Ouyang, X. P., Qiu, X. Q., Lou, H. M., and Yang, D. J. (2006). “Corrosion and scale inhibition properties of sodium lignosulfonate and ins potential application in recirculating cooling water system,” *Ind. Eng. Chem. Res.* 45(16), 5716-5721.
- Ouyang, X. P., Zhang, P., Tan, C. M., Deng, Y. H., Yang, D. J., and Qiu, X. Q. (2010) “Isolation of lignosulfonate with low polydispersity index,” *Chin. Chem. Lett.* 21(12), 1479-1481.
- Qiu, X. Q., Kong Q., Zhou M. S., and Yang, D. J. (2010). “Aggregation behavior of sodium lignosulfonate in water solution,” *J. Phys. Chem. B*, 114(48), 15857-15861.
- Qiu, X. Q., Yang, D. J., and Ouyang, X. P. (2003). “Adsorption of calcium lignosulfonates on surface of solid particle,” *Journal of Chemical Industry and Engineering (China)* 58(4), 1155-1159.
- Ratinac, K. R., Stand, O. C., Bryant, P. J. (2004). “Lignosulfonate adsorption on and stabilization of lead zirconate titanate in aqueous suspension,” *Colloid and Interface Science* 273, 442-454.
- Schärfl, W. (2007). *Light Scattering from Polymer Solutions and Nanoparticle Dispersions*. Pasch, H. (ed.), Springer-Verlag, Berlin.
- Woerner, D. L., and McCarthy, J. L. (1988). “Lignin 24 ultrafiltration and light-scattering evidence for association of kraft lignins in aqueous solutions,” *Macromolecules* 21(7), 2160-2166.
- Yan, M. F., Yang, D. J., Deng Y. H., Chen, P., Zhou, H. F., and Qiu, X. Q. (2010). “Influence of pH on the behavior of lignosulfonate macromolecules in aqueous solution,” *Colloids Surf. A: Physicochemical and Engineering Aspects* 371, 50-58.
- Zhang, Y. L., Qiu, X. Q., Wang, W. X., and Yang, D. J. (2005). “Adsorption performance of lignosulfonates on coal-water interface,” *Journal of South China University of Technology (Natural Science)* 33(6), 51-59.
- Zhou, M. S., Qiu, X. Q., Yang, D. J., Lou, H. M., and Ouyang, X. P. (2007). “High-performance dispersant of coal-water NaSLurry synthesized from wheat straw alkali lignin,” *Fuel Process. Technol.* 88(4), 375-382.

Article submitted: July 22, 2011; Peer review completed; August 31, 2011; Revised version received and accepted: September 25, 2011; Published: September 27, 2011.